日 磁 歯 誌
J J Mag Dent
ISSN 0918-9629

2017 Volume 26. Number 2

JSMAD

日本磁気歯科学会雑誌

The Journal of the Japanese Society
of Magnetic Applications in Dentistry

Volume 26, Number 2

The Japanese Society of Magnetic Applications in Dentistry

日本磁気歯科学会

日本磁気歯科学会雑誌 第二十六巻 第二号 J J Mag Dent 2017 日本磁気歯科学会

The Journal of the Japanese Society of Magnetic Applications in Dentistry

Volume 26, Number 2

Proceedings of the 16th International Conference on Magnetic Applications in Dentistry

The Japanese Society of Magnetic Applications in Dentistry

The 16th International Conference on Magnetic Applications in Dentistry

The 16th International Conference on The Japanese Society of Magnetic Applications in Dentistry organized by JSMAD was held on the Internet as follows;

Meeting Dates:

February 28 to March 17, 2017

Location:

JSMAD web site

http://www.jsmad.jp/international-e.shtml

General Chair:

Prof. Motonobu Miyao, Asahi University

Conference Secretariat:

Masatoshi Iwahori, Asahi University

Subjects:

Researches and developments related to dentistry and magnetism such as:

- Magnetic attachments for dentures
- Orthodontic appliances using magnets
- Measurement of jaw movement using magnetic sensors
- Biological effects of magnetic fields
- Dental applications of MRI
- Others

Conference Committee

The Japanese Society of Magnetic applications in Dentistry

President of the Japanese Society of Magnetic applications in Dentistry

Dr. Shuji Ohkawa, Meikai University

Vice-President of the Japanese Society of Magnetic applications in Dentistry

Dr. Chikahiro Ohkubo, Tsurumi University

Conference Secretary

Dr. Mineyo Sone, Meikai University

Conference Organizing Committee

Dr. Hideki Aita, Health Sciences University of Hokkaido
Dr. Tetsuo Ohyama, Nihon University
Dr. Shunsuke Minakuchi, Tokyo Medical and Dental Universit
Dr. Masatake Akutagawa, The University of Tokushima
Dr. Kazuo Nakamura, Sanno Hospital
Dr. Tetsuo Ichikawa, The University of Tokushima
Dr. Kazuhiro Nagata, The Nippon Dental University
Dr. Tohru Kurabayashi, Tokyo Medical and Dental University
Dr. Masayuki Hideshima, Tokyo Medical and Dental University
Dr. Hisashi Koshino, Health Sciences University of Hokkaido
Dr. Yuji Homada, Homada Shika Daiichi Shinryoujo
Dr. Yukyo Takada, Tohoku University
Dr. Masato Makita, Keitendo Dental Office
Dr. Jun Takebe, Aichi-Gakuin University
Dr. Eri Makihara, Kyusyu Dental University
Dr. Joji Tanaka, Tanaka Dental Clinic
Dr. Tatsuhiko Masuda, Aichi-Gakuin University
Dr. Naoki Tsukimura, Nihon University
Dr. Shinichi Masumi, Kyusyu Dental University
Dr. Fujio Tsuchida, Mami's Dental Office
Dr. Motonobu Miyao, Asahi University

Conference Arrangements Committee

Dr. Masatake Akutagawa, The University of Tokushima
Dr. Tetsuo Ohyama, Nihon University
Dr. Hisashi Koshino, Health Sciences University of Hokkaido
Dr. Yuji Homada, Homada Shika Daiichi Shinryoujo
Dr. Eri Makihara, Kyusyu Dental University
Dr. Juro Wadachi, Tokyo Medical and Dental University

Published by the Japanese Society of Magnetic Applications in Dentistry

c/o Department of Removable Prosthodontics,
Tsurumi University School of Dental Medicine
2-1-3, Tsurumi, Tsurumi-ku, Yokohama 230-8501 JAPAN

B&W: Kisatu α print Co.,Ltd
3Jyo16-1-45, Hiragishi, Toyohira-ku, Sapporo, Hokkaido 062-0933 JAPAN

The 17th International Conference on Magnetic Applications in Dentistry General Information

General Information

The Japanese Society of Magnetic Applications in Dentistry (President: Shuji Ohkawa, Meikai University) is a scientific association founded in 1991 and is devoted to furthering the application of magnetism in dentistry. The 17th International Conference on Magnetic Applications in Dentistry organized by JSMAD will take place on the Internet as follows.

Meeting Dates:

Monday, February 26 to Friday, March 16, 2018

Location:

JSMAD web site:
http://jsmad.jp/international/17/

General Chair:

Assoc. Prof. Yukyo Takada, Tohoku University

Subjects:

Researches and developments related to dentistry and magnetism such as:

- Magnetic attachments for dentures
- Orthodontic appliances using magnets
- Measurement of jaw movement using magnetic sensors
- Biological effects of magnetic fields
- Dental applications of MRI
- Others

Registration Information

Registration:

Send e-mail titled "registration for 17th international conference" with your Name, University or Institution, Postal address, Phone, Fax and E-mail address to conference secretariat.

Registration Fees:

No registration fees. Anyone who is interested in magnetic applications in dentistry can participate in the conference via the Internet.

Publishing Charge for Proceedings:

After the conference, the proceeding will be published. The publishing charge is 10,000 yen per page. (No charge for invited paper.)

Guidelines for Presentation

Deadlines:

Entry: January 26, 2018
Poster submission: February 16, 2018

Entry:

Send Title and Abstract within 200 words with your Registration.

Paper submission:

Please send papers in Microsoft Word format to the conference secretariat by E-mail. All contents should be written in English. No multi-byte character, such as Japanese Kanji, should be contained. A template file can be obtained from the conference web site. Web presentations for the conference will be produced by the secretariat from the paper. The secretariat will not make any correction of the paper even miss-spelling, grammatical errors etc. Alternative format files are acceptable. Please contact to the secretariat for more detailed information.

Discussion:

Discussions will be done using a bulletin board on JSMAD Web Site via the Internet. The authors should check the board frequently during the meeting dates. If questions or comments on your presentation are posted, please answer them as soon as possible.

Notice to Contributors:

Freely-given informed consent from the subjects or patients must be obtained. Waivers must be obtained for photographs showing persons.

Note:

Copyright of all posters published on the conference will be property of the Japanese Society of Magnetic Applications in Dentistry. Copies of the posters will be made and transferred to JSMAD web site for continuous presentation after the meeting dates.
For further information,
send e-mail to meeting27@jsmad.jp

Conference Secretariat

Masatoshi Takahashi, Tohoku University
E-mail: takahashi@m.tohoku.ac.jp
Tel & Fax: 81-22-717-8317

Visit JSDMD Home Page for updates!
http://www.jsmad.jp/

Contents

Optimal structural design evaluation of magnetic attachments using a three-dimensional finite element method

H Nagai[1], H Kumano[1], R Kanbara[1], T Itakura[1], K Hayashi[1], A Ando[1], T Masuda[1], Y Nakamura[1], Y Takada[2], Y Tanaka[1], and J Takebe[1]

[1]Department of Removable Prosthodontics, School of Dentistry, Aichi-Gakuin University
[2]Division of Dental Biomaterials, Tohoku University Graduate School of Dentistry

Abstract

Magnetic attachments are designed to exert an attractive force at clinically useful levels. However, improving the attractive force is necessary in order to deal with complex clinical conditions. The present study analyzed and investigated magnetic attachments from the point of a magnetic circuit using a three-dimensional finite element method to enhance their performance.

An analysis model was constructed based on a dental magnetic attachment (GIGAUSS D 600, GC). In the analysis model, a round, non-magnetic material was embedded in 1) the disk yoke only, 2) the keeper only, and 3) both the disk yoke and the keeper. The magnetic flux density distribution and attractive force were analyzed by changing the diameter of the non-magnetic material by 0.05 mm.

An increase in the magnetic flux density on the attractive surface was confirmed by embedding a non-magnetic material in the magnetic assembly and the keeper. However, the magnetic flux density was oversaturated when it exceeded a certain value. A similar tendency was observed in the attractive force.

Introduction

Magnetic attachments have continued to improve. Various magnetic circuits have been designed so that the minimal amount of magnetic attachment can exert a high attractive force.

A magnetic attachment consists of a magnet assembly and a keeper. A magnet in the magnetic assembly is encapsulated by magnetic and non-magnetic materials. Magnetic flux can penetrate a magnetic body but cannot penetrate non-magnetic material. Magnetic flux is the magnetic line of force. It penetrates magnetic materials and forms a closed magnetic circuit that exerts an attractive force when a magnetic assembly and a keeper come into contact.[1)]

Attractive force is affected by the attractive surface area of a magnetic assembly and a keeper and the magnetic flux density. Since the size of a magnetic attachment should be minimal, it is impossible to increase the attractive surface area of a magnetic assembly and a keeper.[2)] The attractive force of a magnetic attachment can be effectively increased by increasing the magnetic flux density. A magnetic

circuit changes by incorporating non-magnetic material in the inner structure of a magnetic assembly and a keeper; this may increase the magnetic flux density. In other words, clinically feasible magnetic assemblies and keepers can be developed by introducing an optimal magnetic circuit. The finite element method is considered the most effective for optimizing the magnetic circuit, as it can visualize the dynamic behavior of the magnetic circuit inside a magnet, and simulations can be performed by changing the conditions.

Objective

A three-dimensional finite element method was used to analyze the influence of differences in the magnetic circuit on the attractive force and to optimize the magnetic circuit by changing the internal structure of the magnetic attachment.

Materials and Methods

1. *Analysis model*

The size of the magnetic assembly was 1.8 mm in radius and 1.3 mm in height. The magnet inside the magnetic assembly was round with a radius of 1.3 mm and 0.5 mm in height. The size of a ring was 0.2 mm in width and 0.2 mm in height. A disk yoke had a radius of 1.1 mm and a height of 0.2 mm. The keeper was round, with a radius of 1.8 mm and a height of 0.7 mm. Considering that the model was axially symmetrical, the basic model was set at 1/4 scale (Fig. 1).

The analysis range was 2.0 mm around the magnetic assembly and keeper. Marc Mentat 2010 (Multi-Purpose Finite Element Pre- and Post-Processor, MSC) was used for model construction, using μ-MF (electromagnetic field analysis system, μ-TEC) analysis software. Elements were three-dimensional pentahedrons and hexahedrons. The element count was 53,802, and the nodal point count was 57,784.

The components of the magnet were Nd-Fe-B (Neodymium, Ferrum, Boron), and its magnetic properties were calculated based on the thermal property of GIGAUSS D 600 and values provided by the manufacturer.[3] The components of the yoke and keeper were measured by the magnetic properties of SUSXM27, and the B-H curves of the magnetic properties were calculated by the approximation formula (Table 1).

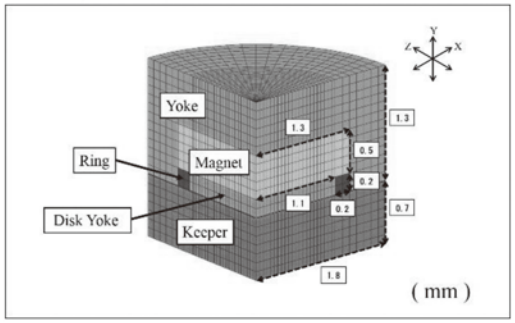

Fig. 1 Basic model

Table 1 Analysis conditions

Magnet		
Nd-Fe-B	(BH) max = 46 MGOe Residual magnetic jnduction = 1. 22 T	
Keeper & Yoke		
SUS XM27	Saturation magnetic induction = 1. 35 T	
B-H curve	$B = Bs \{ 1 - \exp (-\mu_r \cdot \mu_0 \cdot H / Bs) \}$	

2. *Analysis items*

(1) Disk yoke only

Non-magnetic material was embedded at the center of the disk yoke of a magnetic assembly and the center of the attractive surface of a keeper. The radius of the non-magnetic material was changed in 0.05 mm increments from 0.05 mm to 1.0 mm at the center of a disk yoke (20 patterns in total) (Fig. 2).

(2) Keeper only

At the center of the attractive surface of a keeper, the radius of the non-magnetic material was changed in 0.05 mm increments from 0.05 mm to 1.0 mm, and the depth was changed by 0.1 mm from 0.1 mm to 0.6 mm (120 patterns in total) (Fig. 3).

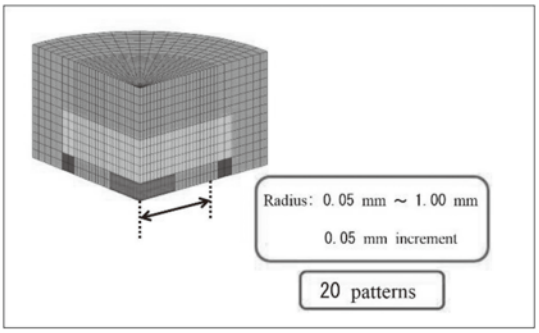

Fig. 2 Analysis item

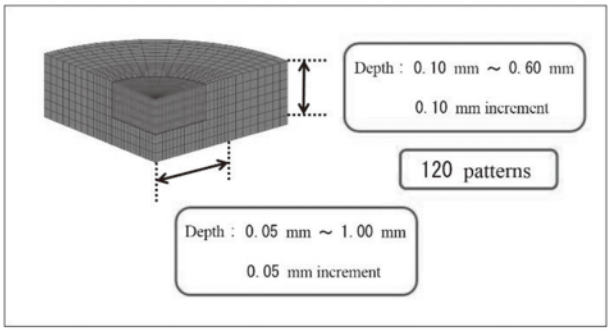

Fig. 3 Analysis item

(3)Both the disk yoke and keeper

Parts of (1) and (2) were combined, and a total of 1,200 patterns were analyzed (Fig. 4).

Analysis results were evaluated as the magnetic flux density and the attractive force.

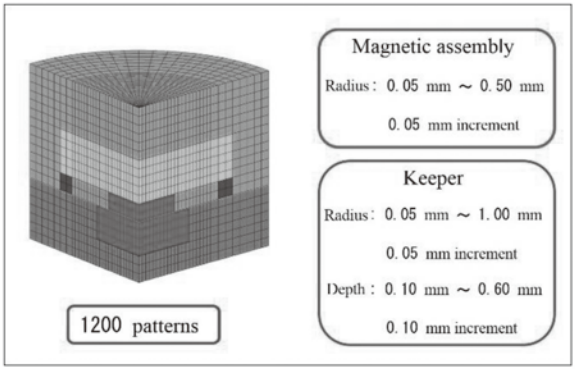

Fig. 4 Analysis item

Results

Attractive force and magnetic flux density distribution

(1) Disk yoke only

A graph of the attraction force of the analysis result is shown (Fig. 5). A gradual increase in the attractive force was observed. The attractive force reached a maximum of 560 gf when the radius of the non-magnetic material at the center of the disk yoke was 0.3 mm, but it decreased thereafter as the radius of the non-magnetic material increased.

Representative magnetic flux density distribution is shown in Fig. 6. An increase in the magnetic density was confirmed in the magnetic assembly and the attractive surface of a keeper. When the radius of the non-magnetic material at the center of the disk yoke exceeded 0.3 mm, the magnetic flux density in the magnetic assembly and on the attractive surface of the keeper became oversaturated, and a decrease in the magnetic flux density in the magnetic assembly and within the keeper was observed.

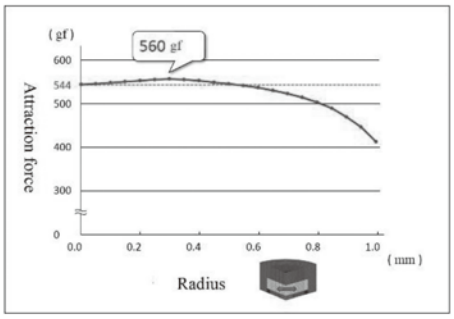

Fig. 5 Attraction force

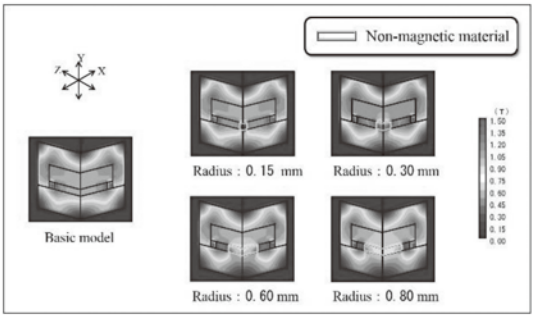

Fig. 6 Magnetic flux density distribution

(2)Keeper only

A graph of the attraction force of the analysis result is shown (Fig. 7). A gradual increase in the attractive force was observed. The attractive force reached a maximum of 582 gf when the radius of the non-magnetic material at the center of the keeper was 0.6 mm, but it decreased thereafter, with an increased radius of the non-magnetic material. There was little influence on the depth of the non-magnetic material until its radius at the center of the keeper's attractive surface reached 0.6 mm, where the attractive force continued to increase.

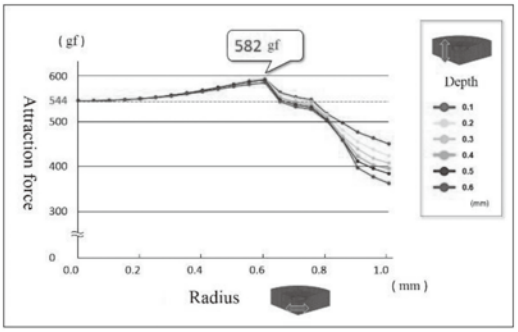

Fig. 7 Attraction force

Representative magnetic flux density distribution is shown (Fig. 8). An increase in the magnetic density was confirmed in the magnetic assembly and the attractive surface of the keeper. When the radius of the non-magnetic material at the center of the keeper's attractive surface exceeded 0.6 mm, the magnetic flux density in the magnetic assembly and on the attractive surface of the keeper became oversaturated, and a decrease in the magnetic flux density in the magnetic assembly and within the keeper was observed.

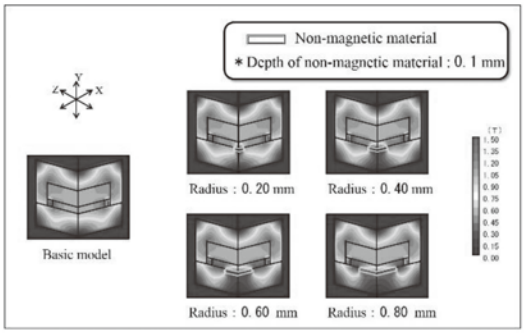

Fig. 8 Magnetic flux density distribution

(3) Both the disk yoke and keeper

A graph of the attraction force of the analysis result is shown (Fig. 9). This is influenced by the radius

of the non-magnetic material embedded in the keeper's attractive surface on the attractive force at the depth where the radius of the non-magnetic material at the center of a disk yoke was 0.15 mm. There was no influence on the depth until the radius of the non-magnetic material in the keeper's attractive surface reached 0.5 mm. The attractive force was highest when the radius was 0.5 mm. When the radius exceeded 0.55 mm, the attractive force started to decrease and was affected by the depth.

A graph of the attraction force of the analysis result is shown (Fig. 10). This is influenced by a change in the radius of the non-magnetic material in the keeper's attractive surface on the attractive force at the center of a disk yoke. Since the depth of the non-magnetic material had little influence until the radius of the non-magnetic material at the center of the keeper's attractive surface reached 0.5 mm where the attractive force continued to increase (Fig. 9), the depth of the non-magnetic material was set at 0.1 mm. The attractive force increased as the radius of the non-magnetic material at the center of the keeper's attractive surface increased. The attractive force reached a maximum of 598 gf when the radius of the non-magnetic material was 0.15 mm and that of the keeper was 0.5 mm; however, it decreased thereafter as the radius of the non-magnetic material on the attractive surface of the keeper increased.

The representative magnetic flux density distribution is shown (Fig. 11). This is the radius of the non-magnetic material at the center of the attractive surface of a keeper that was changed when the radius of the non-magnetic material at the center of the disk yoke was 0.15 mm, and the depth of the non-magnetic material at the center of the attractive

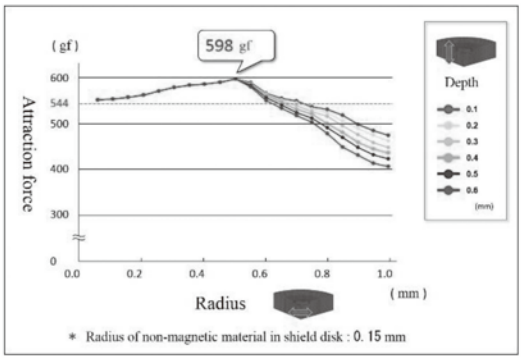

Fig. 9 Attraction force (Influence of the depth)

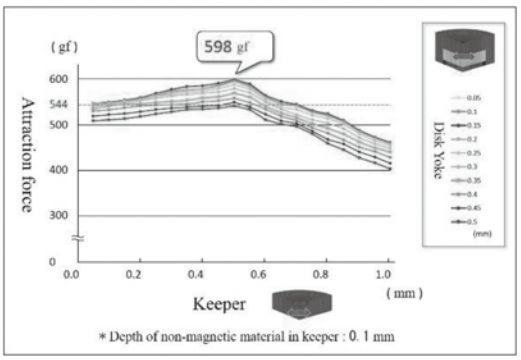

Fig. 10 Attraction force
(Influence of disk yoke and keeper)

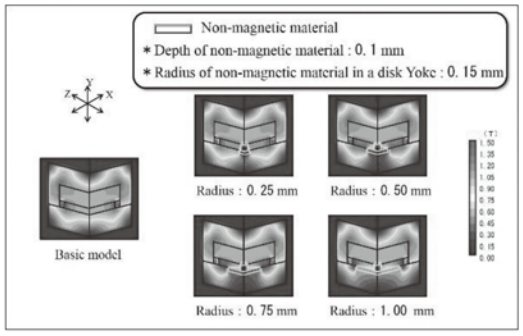

Fig. 11 Magnetic flux density distribution

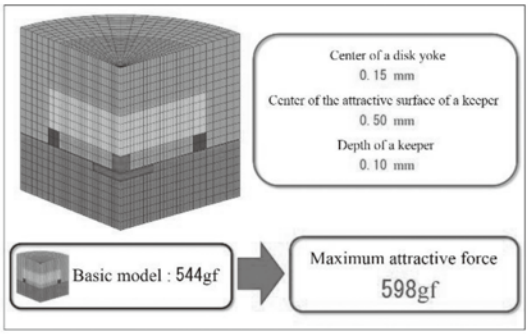

Fig. 12 Optimal structural design model

surface of the keeper was 0.1 mm.

An increase in the magnetic density was confirmed in the magnetic assembly and attractive surface of the keeper. When the radius of the non-magnetic material at the center of the attractive surface of the keeper exceeded 0.75 mm, the magnetic flux density of the magnetic assembly and on the attractive surface of the keeper became oversaturated, and a decrease in the magnetic flux density in the magnetic assembly and inside the keeper was observed.

From the analysis results so far, when the attractive force of the basic model was defined as 100%, the attractive force increased to approximately 110% at a radius of 0.15 mm of the non-magnetic material at the center of the disk yoke, a radius of 0.5 mm of the non-magnetic material at the center of the attractive force of a keeper, and a depth of 0.1 mm of the non-magnetic material in a keeper where the attractive force reached the maximum (Fig. 12).

Discussion

1. Efficiency of the finite element method

It is difficult to measure and observe details of the behavior of the attractive and repelling forces created by a magnet. This is because the magnetic field has a gradient in all directions, and, therefore, a simple calculation formula cannot be established. The finite element method allows the visualization and simulation of the inner behavior of the magnetic circuit by adding various conditions. It is considered time efficient and cost-effective to search the optimal magnetic circuit using the finite element method.

2. The relationship between the attractive surface area and the magnetic flux density

The attractive force of a magnet can be expressed as $F = (1/2\mu_0) \cdot S \cdot B^2$ {μ_0: space permeability, S: attractive surface area, B: magnetic flux density}.[4] The attractive force of a magnetic attachment is affected more by the magnetic flux density than by the attractive surface area.[5] Therefore, the attractive force can be increased efficiently by increasing the magnetic flux density. The magnetic circuit changes by replacing part of a keeper of a magnetic attachment with a non-magnetic material, resulting in an increase in the magnetic flux density on the attractive surface. The attractive force was affected more by an increase in the magnetic flux density than by a decrease in the attractive surface area, resulting in an increase in the attractive force. However, there is a limit to the magnetic flux density in the magnetic body, called “saturated magnetic flux density.” When the magnetic body reaches that point, the increase in the magnetic flux density stops, even when the size of the non-magnetic material continues to increase. As a result, the attractive force decreases, due to the influence of the attractive surface area. The relationship between the attractive surface area and the magnetic flux density is extremely important for optimizing the magnetic circuit.

3. Inferring the depth

The attractive force is affected by an increased magnetic flux density on the attractive surface, and it

is rarely affected by the depth of the non-magnetic material. However, when the radius of the non-magnetic material at the center of an attractive surface of a keeper exceeds 0.5 mm, the magnetic flux density on the attractive surface becomes oversaturated. The magnetic flux that could not penetrate the attractive surface flows into the non-magnetic material. The magnetic flux has difficulty penetrating the non-magnetic material; however, a small amount of magnetic flux can flow. The deeper the non-magnetic material gets, the more difficulty the magnetic flux has penetrating the non-magnetic material. A decrease in the attractive force is considered to be caused by the depth of the non-magnetic material.

Conclusion

Optimal structural design evaluation of magnetic attachments was analyzed and investigated using a three-dimensional finite element method, and the following results were obtained:

1. An increase in the attractive force was confirmed by setting a non-magnetic material inside the magnetic attachment and changing the magnetic circuit.
2. It was confirmed that the increase in the attractive force was greater when the non-magnetic material was set at the center of an attractive surface of a keeper than at the center of a disk yoke of the magnetic assembly.
3. The influence of the depth of non-magnetic material at the center of an attractive surface of a keeper was small compared to the size of the radius.

References

1. Y Kinouchi: Fundamental physical properties of magnetic attachment, Sika Journal, 17–26, 1993.
2. O Okuno: Structure and characteristics of magnetic attachments, Tohoku Univ. Dent. J., 13: 1–10, 1994.
3. T Miyata, J Niimi, A Ando, et al.: Influence of heating of a magnetic attachment on the attractive force, J. J. Mag. Dent., 17: 44–50, 2008.
4. Y Nakamura: Stress analysis of an overlay denture and a magnetic attachment using finite element method, Nihon Hotetsu Shika Gakkai Zasshi, 42(2), 234–245, 1998.
5. H Kumano, Y Nakamura, R Kanbara, et al.: A three-dimensional finite element evaluation of magnetic attachment attractive force and the influence of the magnetic circuit, Dent. Mater. J., 33(5), 669–673, 2014.

Effect of horizontally shifting the center of the magnetic assembly and that of the keeper on the retentive force of cup-yoke dental magnetic attachments

M. Takahashi, H. Sakatsume, M. Kanyi and Y. Takada

Division of Dental Biomaterials, Tohoku University Graduate School of Dentistry

Abstract

It is generally known that the retentive force of dental magnetic attachments decreases in the presence of a gap. In this study, the retentive forces of cup-yoke type magnetic attachments in different horizontal positions, were measured and the relationship investigated. The mechanism leading to the change was studied by making use of models.

The three dental magnetic attachments used were: GIGAUSS, HYPER SLIM and an experimental set made of HYPER SLIM magnetic assembly paired up with a keeper which had a hole at the center. Retentive forces were measured as per ISO 13017, in various positions whereby the center of magnetic assembly and that of the keeper was shifted horizontally at intervals of 100 μm.

Retentive forces of all the sets decreased with increase in horizontal displacement. The decrease was not uniform and the curve had many inflection points. Based on analysis using mathematical formulas, conclusions could be made as follows: 1. Retentive force changes due to movement of magnetic assembly away from the keeper though the actual determinant is the disparity in contact surface area between cup-yoke to keeper and keeper to disk-yoke. 2. The change in contact surface area affects fields in the closed magnetic circuit leading to reduced retentive forces.

Introduction

It is well known that the retentive force of a dental magnetic attachment decreases with the presence of a vertical gap between mating surfaces, which may occur due to an air gap erroneously introduced into the magnetic assembly during the fixation of a magnetic attachment into a removable denture.[1] The three-dimensional finite element method of analysis and some rough measurements show that even in the absence of a gap between the mating surfaces, any horizontal displacement between the magnetic assembly and the keeper reduces the retentive force.[2,3] However, no available research shows the detailed relationship between the horizontal displacement and the retentive force.

There are two types of magnetic attachments based on magnetic circuits: open and closed. The open magnetic circuit type has a retentive force that is directly proportional to the area of mating faces in contact; however, this type of attachment is hardly used. In contrast, the closed magnetic circuit type does not have a retentive force that is directly proportional to the contact surface area. This is due to the influence of the magnetic flux direction on the retentive force; this type of attachment is mainly used in Japanese products. A proper understanding of the retentive force change mechanism is useful for developing a magnetic attachment and the appropriate technique for clinical purposes.

Objective

In this study, the retentive forces of cup-yoke type dental magnetic attachments were measured in different horizontal positions and the relationship between the retentive force and horizontal displacement was investigated. The mechanism leading to the changes in retentive force was studied by means of modeling.

Materials and Methods

Three dental magnetic attachments were used: GIGAUSS D600 (GC), HYPER SLIM 3513 (Morita), and an experimental set (hereafter named Hollow Keeper) based on a HYPER SLIM magnetic assembly paired with a keeper (ϕ 3.5 mm) made of SUS XM27 bearing a ϕ 1.4 mm hole at the center. A measuring device that matched ISO 13017:2012/Amd.1:2015[4,5] was connected to a digital force gauge (ZPS, Imada). Retentive forces were measured at a crosshead speed of 5 mm/min according to ISO 13017 in various positions wherein

the center of the magnetic assembly and that of the keeper were shifted horizontally (horizontal displacement) at intervals of 100 μm.

Simplified models of the magnetic attachments were used to assist in calculating the contact surface area between the cup-yoke and the keeper and between the disk-yoke and the keeper in different positions. The values derived from mathematical projections and calculated by formulas were compared with the actual values.

Results

Dependencies of the retentive force on the horizontal displacement are shown in Fig. 1 for GIGAUSS, HYPER SLIM and Hollow Keeper. Retentive forces for all three types decrease as horizontal displacement increases. The dependency was not linear and had several inflection points. The curve lines for the retentive force versus the displacement for GIGAUSS and HYPER SLIM were smooth in contrast to that for Hollow Keeper, which had a single odd point slightly above 2 mm of displacement.

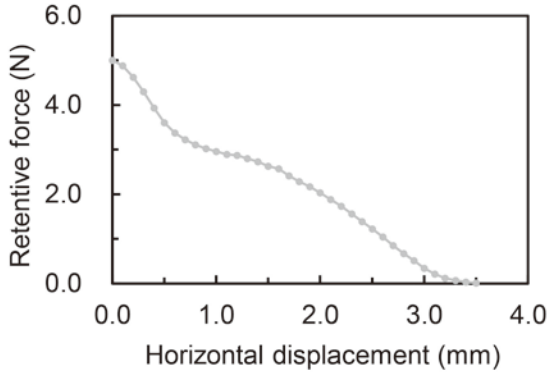

a: GIGAUSS

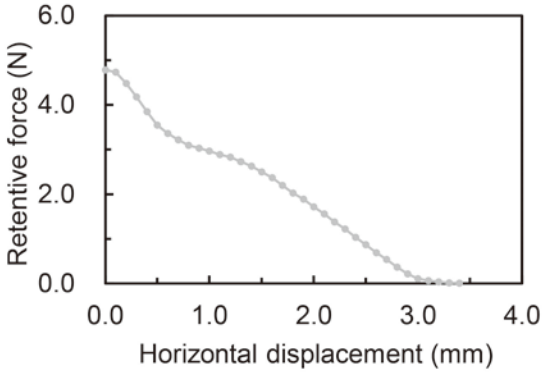

b: HYPER SLIM

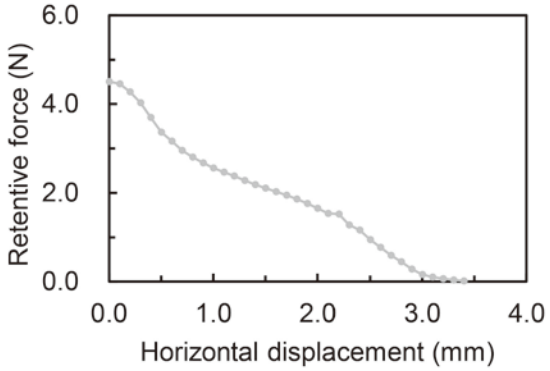

c: Hollow Keeper

Fig. 1 The retentive force against the horizontal displacement

Discussion

1. Internal structure of dental magnetic attachments

To analyze the retentive force of a magnetic attachment, it is important to know the internal structure of magnetic attachments beyond the information disclosed by the manufacturer. A simple model of magnetic attachments for illustration of internal structure is shown in Fig. 2, where r is the radius of the magnetic assembly and keeper, a is the radius of the disk-yoke, b is the thickness of the shield ring (spacer), $c = a + b$ is the radius of the disk-yoke and thickness of the shield ring, and d is the radius of the hole in the Hollow Keeper.

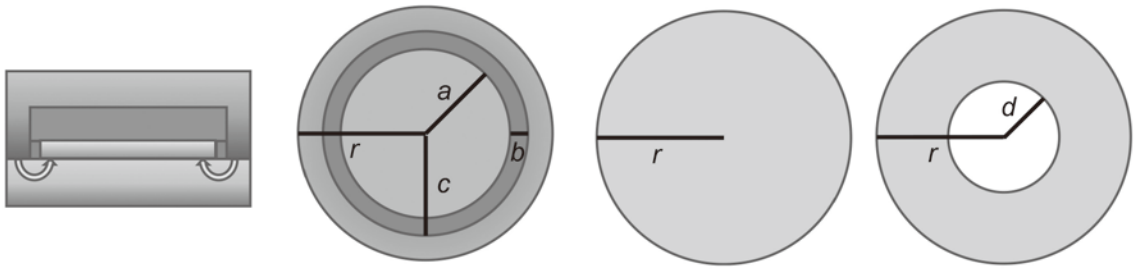

a: Magnetic attachment transverse view | b: Magnetic assembly | c: Keeper surface view | d: Hollow Keeper

Fig. 2 Simple model of magnetic attachments

The magnetic attractive force (F) is calculated using equation (1), where C is the constant, B is the magnetic flux density, and S is the surface area. Increasing the magnetic flux density enhances the magnetic attractive force, as compared to a similar increase in the surface area of a mating surface.

$$F = C \times B^2 \times S \quad (1)$$

Since a strong neodymium magnet was used in all the sets in this study, the magnetic flux density at the cup-yoke surface was predominantly saturated. Therefore, the cup-yoke surface area was the main determinant of the retentive force. Magnetic flux begins on the cup-yoke and returns to the magnet through the disk-yoke. To optimize this effect, the design should be geared toward a cup-yoke, which has a surface area (S_{cup}) equal to or slightly smaller than that of a disk-yoke (S_{disk}).

$$S_{cup} = \pi r^2 - \pi(a+b)^2 \quad (2)$$
$$S_{disk} = \pi a^2 \quad (3)$$
$$S_{cup} \leq S_{disk} \quad (4)$$

As an illustration, GIGAUSS has an outer diameter of 3.6 mm (radius is 1.8 mm), and a shield ring generally is 0.15~0.2 mm thick.[2, 3] Thus $r = 1.8$, and $b = 0.2$. After substituting the above values into equations (2-4), one obtains $a \geq 1.169$. The thickness of the cup-yoke $\{r - (a + b)\}$ is 0.4 mm, whereas the radius of the disk-yoke is 1.2 mm. In a similar way, for HYPER SLIM ($r = 1.75$ and $b = 0.2$), one can calculate the thickness of the cup-yoke as 0.4 mm and the radius of the disk-yoke as 1.15 mm.

2. Calculation of the contact surface area between magnetic assembly and the keeper

Since the retentive force of the magnetic attachment was dependent on the contact surface area between the magnetic assembly and the keeper, we calculated the contact surface area for the horizontal displacement. The horizontal displacement (t) represents the distance between the center of the magnetic assembly and that of the keeper, which was calculated using equation (5). The central angle, θ, is formed by the intersection of two lines drawn from the center of either the keeper or the magnetic assembly to each of the two points where the outer margins of the keeper and the assembly intersect (Fig. 3a).

$$t = 2r\cos\frac{\theta}{2} \quad (5)$$

t and t' in Fig. 3a correspond to the shifting movement of the assembly or the keeper. Wherein $\theta: \pi \rightarrow 0$ in equation (5), $t: 0 \rightarrow 2r$. The overlap decreases until the assembly and the keeper eventually separate completely (Fig. 3a).

Two additional equations were derived in order to calculate the contact surface area of the magnetic assembly in contact with the keeper at different positions based on the displacement. Equation (6) is based on Fig. 3b, which illustrates a certain position when area S_{rr} is formed by two components with the same radii (r) at distance t.

$$S_{rr} = \pi r^2 \frac{\theta}{2\pi} \times 2 - r \cdot r\sin\theta = r^2(\theta - \sin\theta) \quad (6)$$

Equation (7) is based on Fig. 3c, which illustrates a certain position in which area S_{cr} was formed by two circles with different radii (r, c) at distance t.

$$S_{cr} = c^2\theta' + r^2\theta'' - t \times c\sin\theta' = c^2\cos^{-1}\left(\frac{t^2+c^2-r^2}{2tc}\right) + r^2\cos^{-1}\left(\frac{t^2-c^2+r^2}{2tr}\right) - \frac{\sqrt{4t^2c^2-(t^2+c^2-r^2)^2}}{2} \quad (7)$$

$$\because \cos\theta' = \frac{t^2+c^2-r^2}{2tc}, \qquad \cos\theta'' = \frac{t^2-c^2+r^2}{2tr}, \qquad \sin^2\theta' + \cos^2\theta' = 1$$

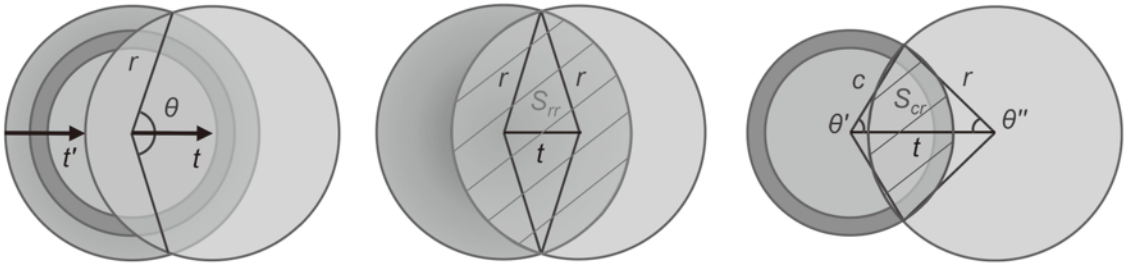

a: Horizontal displacement t and central angle θ b: Same radius size c: Different radius size

Fig. 3 Calculation of the contact surface area in various positions of displacement

3. Contact surface area of GIGAUSS and HYPER SLIM

Since the retentive force of the cup-yoke-type magnetic attachment was relatively dependent on the area of the cup-yoke surface in contact with the keeper, the area values were calculated at three different positions of horizontal displacement as a result of shifting either the keeper or the assembly laterally. Figure 4 shows equations for calculating surface area $S_{cup}1$-3 corresponding to horizontal displacements $t1$-3.

$$S_{cup}1 = r^2(\theta - \sin\theta) - \pi c^2 \quad (8)$$

$$S_{cup}2 = r^2(\theta - \sin\theta) - \left\{c^2\cos^{-1}\left(\frac{t^2+c^2-r^2}{2tc}\right) + r^2\cos^{-1}\left(\frac{t^2-c^2+r^2}{2tr}\right) - \frac{\sqrt{4t^2c^2-(t^2+c^2-r^2)^2}}{2}\right\} \quad (9)$$

$$S_{cup}3 = r^2(\theta - \sin\theta) \quad (10)$$

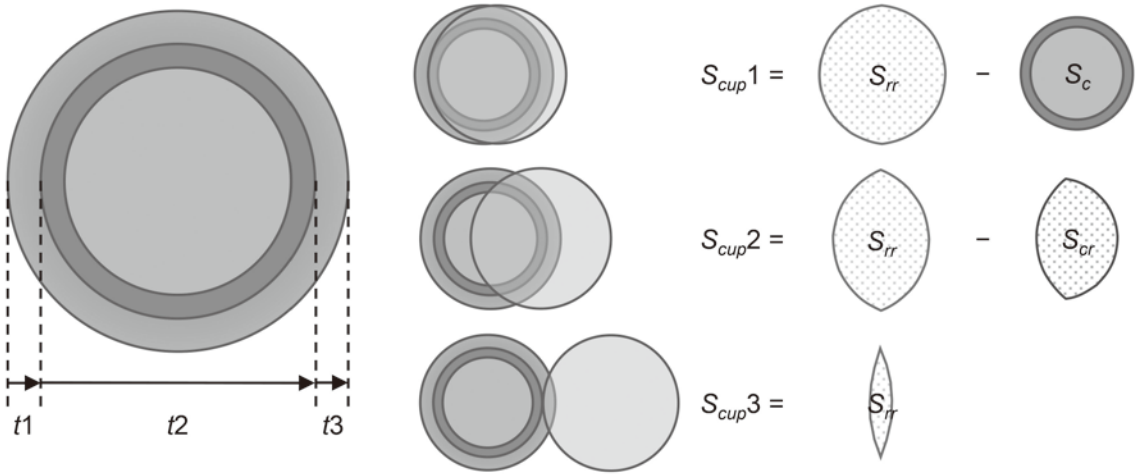

Fig. 4 Schematic diagram for calculating the surface area of a cup-yoke in contact with a keeper in different positions

Values obtained from equations (2-4) for both GIGAUS and HYPER SLIM were substituted into equations (8-10), and the obtained values were plotted on a graph, as shown in Fig. 5a or 5b (blue lines).

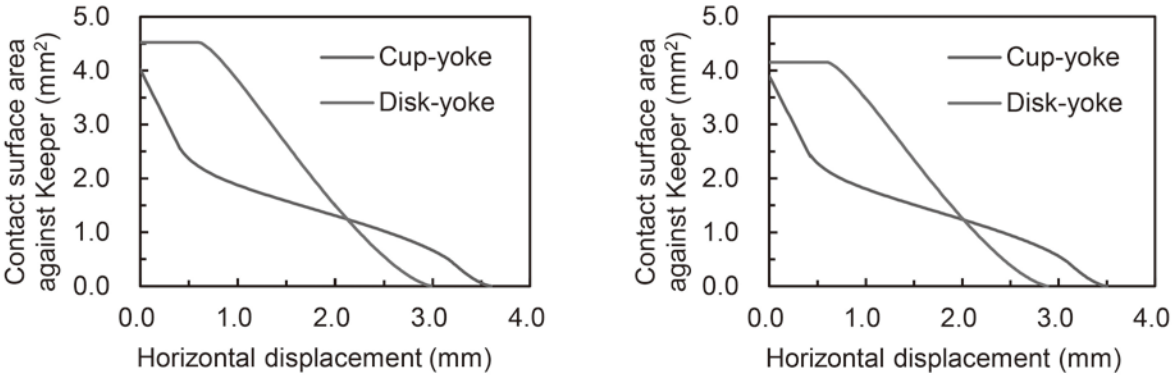

Fig. 5 Contact surface areas against the horizontal displacement

Although the general view of the cup-yoke curve lines is similar to the retentive force in Fig. 1 for values less than 2 mm, the difference becomes apparent for values above 2 mm. This is due to the fact that the surface area between the cup-yoke and the keeper is not the only factor that determines the functionality of a closed magnetic circuit. Therefore, the dependence of the area of the disk-yoke surface in contact with the keeper (S_{disk}1-3) on horizontal displacement (t1-3) was determined as shown in Fig. 6, using the following equations.

$$S_{disk}1 = \pi a^2 \tag{11}$$

$$S_{disk}2 = a^2 \cos^{-1}\left(\frac{t^2+a^2-r^2}{2ta}\right) + r^2 \cos^{-1}\left(\frac{t^2-a^2+r^2}{2tr}\right) - \frac{\sqrt{4t^2a^2-(t^2+a^2-r^2)^2}}{2} \tag{12}$$

$$S_{disk}3 = 0 \tag{13}$$

The values obtained for GIGAUS and HYPER SLIM were substituted into equations (11-13), and obtained values were plotted on a graph as shown in Fig. 5a or 5b (magenta lines).

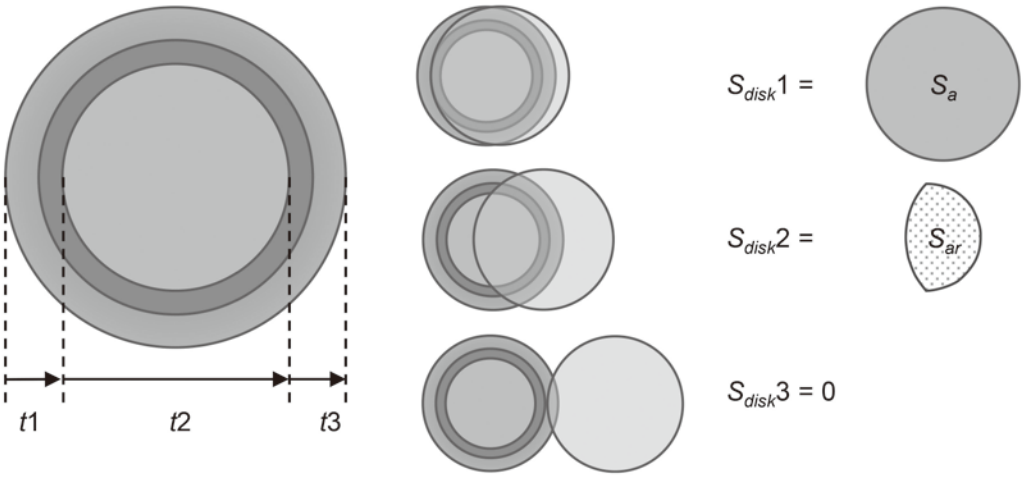

Fig. 6 Schematic diagram for calculating the surface areas of a disk-yoke in contact with a keeper

Magnetic flux from the cup-yoke passes through the keeper and returns to the magnet via the disk-yoke in a closed magnetic circuit system. When the surface area of the contact between the disk-yoke and the keeper is smaller than that between the cup-yoke and the keeper, the magnetic flux that exits through the cup-yoke does not return back, as in the case of a closed magnetic circuit. In such a case, the total retentive force is a function of both closed and open magnetic circuit systems. Therefore, the effect of the surface area on the retentive force should be considered in a relative manner. The resulting surface area related to the total magnetic circuit effect is designated as "S_{mag}." When the contact surface area between the cup-yoke and the keeper is smaller than that between the disk-yoke and the keeper, the magnetic circuit works absolutely as a closed magnetic circuit, and S_{mag} is equal to S_{cup}. The value of the retentive force in a closed magnetic circuit is 2-4 times larger than that of an open magnetic circuit. The influence the area has on the retentive force in

an open magnetic circuit is 1/3 of a closed magnetic circuit. Therefore, S_{mag} can be calculated using equation (14) in a case when the surface area of contact between the cup-yoke and the keeper is larger than that between the disk-yoke and the keeper.

$$S_{mag} = S_{disk} + \frac{S_{cup} - S_{disk}}{3} \quad (14)$$

The resulting surface area (S_{mag}) values were converted to retentive forces. The conversion was based on the S_{mag} value and actual measured force value at a position where $t = 0$ (without displacement), and then plotted as shown in Fig. 7. The similarity in the shape of the curves indicates that the retentive force is dependent on the contact surface area, which influences the magnetic circuit. In general, the actual measured values were higher than those generated using values from projected calculations. This is probably due to the leakage of the magnetic flux from the cup-yoke through a portion of an area that does not contact the keeper.

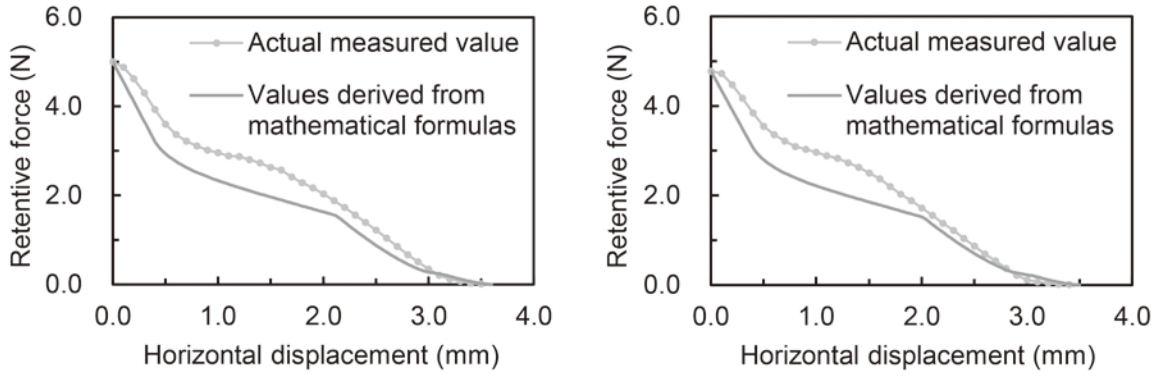

Fig. 7 Retentive force against the horizontal displacement

4. Contact surface area of the Hollow Keeper

Calculating the contact surface area in the case of the Hollow Keeper is quite complex, as illustrated in Fig. 8. The contact surface areas between the magnetic assembly and the keeper in various positions of displacement were plotted on a graph and are shown in Fig. 9a as blue and magenta lines for the cup-yoke and disk-yoke, respectively. It is remarkable that, at certain positions of displacement, the contact surface area of either the cup-yoke or the disk-yoke against the keeper increased with an increase in the horizontal gap. Similarly, when the area of the disk-yoke in contact with the keeper was smaller than that of the cup-yoke in contact with the keeper, the resulting surface area related to the total magnetic circuit (S_{mag}) was calculated using equation (14). Both derived and actual values were represented on a graph are shown in Fig. 9b. In general, the shapes of the two curves are similar. There was a peculiar point (≈ 2.1 mm) on the graph when the curve based on derived values showed a spike. This represents the position where the retentive force based on S_{mag} increased with an increase in the horizontal gap. The spike corresponded with a previously noted odd point on the curve of the actual measured values. This proves that the retentive force is influenced by the resulting contact surface area related to a magnetic circuit. The reason for the large difference between the actual and calculated values at $t = 1.0$~2.0 probably lies in the effect of the magnetic flux leakage through the hole that exists in the keeper in that displacement range.

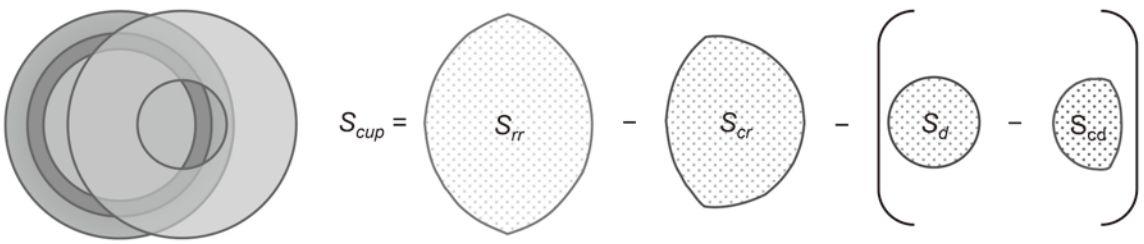

Fig. 8 Schematic diagram for calculation of surface areas of the cup-yoke in contact with the Hollow Keeper

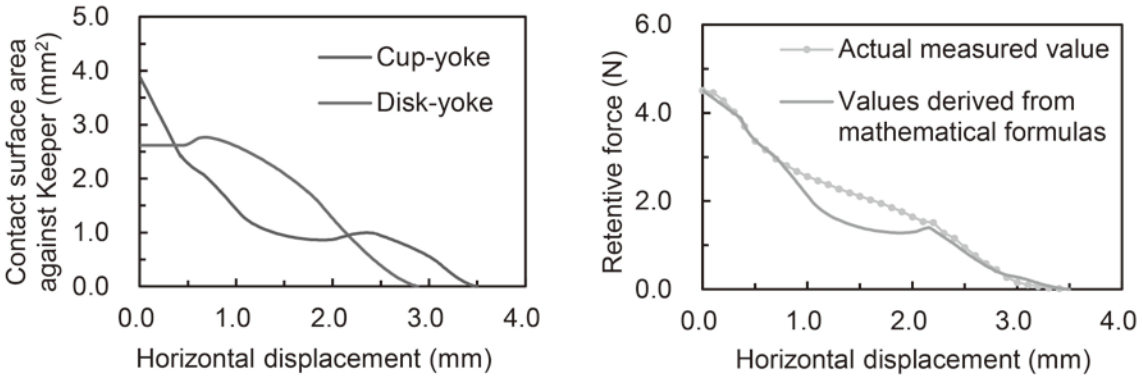

a: Contact surface area b: Retentive force

Fig. 9 Contact surface areas and retentive force of the Hollow Keeper against horizontal displacement

Conclusion

The retentive force of all sets decreases as the horizontal displacement increases. The decrease was not uniform, and the curve had several inflection points. Analysis carried out by means of mathematical formulas demonstrates that the retentive force is influenced by the contact surface area between the cup-yoke and the keeper, as well as the disk-yoke and the keeper, which determine the resulting contact surface area in the magnetic circuit.

References

1. Y. Tanaka, New Dental Magnetic Attachment, pp 2-90, Ishiyaku Publishers, Inc., Tokyo, 2016.
2. H. Nagai: Evaluation of the optimal structural design of magnetic attachments using a three-dimensional finite element method, J J Mag Dent, 25(1), 62-72, 2016.
3. O. Okuno, Y. Takada, K. Nakamura, H. Mizutani, M. Ai, Y. Kinouchi, H. Yamada and H. Suzuki: Improvements of the cup yoke magnetic attachment by use of a thinner shield ring, J J Mag Dent, 2(1), 1-10, 1993.
4. ISO 13017:2012. Dentistry—Magnetic attachments.
5. ISO 13017:2012/Amd.1:2015 Dentistry — Magnetic attachments.

A case report of an implant overdenture using Magfit SX2®

K. Hasegawa, K. Sakakibara, S. Hirota, K. Shimamoto,
R. Watanabe, H. Yamamoto, M. Iwahori and M. Miyao

Department of Prosthodontics, Division of Oral Functional Sciences and Rehabilitation, Asahi University School of Dentistry

Abstract

A 76-year-old man with a chief complaint of a masticatory disturbance with his upper denture came to our hospital in September 2010. Although we fabricated the upper acrylic resin base denture, the patient was not satisfied. Then, after consulting, we fabricated an implant overdenture.

In the case of an implant overdenture, it is difficult to get a well-balanced adjustment for the amount of tissue displacement between the mucosal surface and the implant abutment. In some cases, the attachment may not obtain suction due to the mucous membrane. Magfit SX2®, which was used in this case, has a 0.4 mm range of motion, which is approximately the amount of tissue displacement. We fabricated the implant overdenture with Magfit SX2® using this procedure in order to take advantage of this attachment' s characteristics and shorten the treatment time.

Four years have passed since the insertion of this denture; it has functioned well, and the patient is currently satisfied. It seems this method can easily balance the amount of tissue displacement.

Introduction

Magnetic attachments have been medically approved and quarter a century became common as an abutment device for dentures, and it has also qualified for national exams of dentistry. When using a natural tooth as an abutment, there is the potential for interference equal to a displacement amount of about 70 μm due to the periodontal ligament. However, with an osseointegrated oral implant abutment, adjustment of the displacement amount of the mucosa and the pressure of the implant often depends on the clinical experience, such as design, implant implantation position, and impression pressure.

Magfit SX2®
(Self-adjusting type)

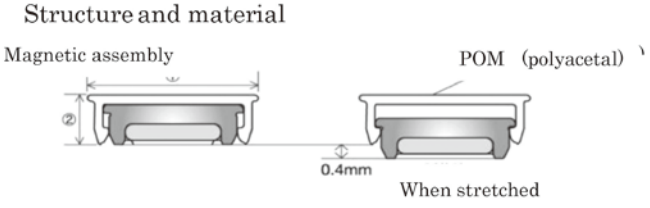

The cap can be inclined by 0.4 mm or 8° in the vertical direction according to the movement of the denture. The fitting force of the cap is about 15 Kgf.

This figure shows the schematic diagram of a Magfit SX2® (self-adjusting type) that has a loose pressure capability, which was used this time. In this issue, we will introduce the method of denture fabrication taking the Magfit SX2® into consideration for adjusting the pressure displacement amount.

Outline of the case

A 76-year-old man with a chief complaint of masticatory disturbance with his upper denture came to our hospital in September 2010. He hoped to obtain a new denture, because the upper complete denture that was made three years ago was not able to chew much. His past history included a cholecystectomy and the ossification of the posterior longitudinal ligament. He was using an upper complete denture that had no spillway and an anti-Monson curve condition. Moreover, because the denture margin was short, due to posterior osteoporosis, I made an upper-jaw resin denture at the patient' s request. However, he was not satisfied; therefore,

I decided to produce a magnetic implant overdenture with the implant.

X-ray photograph before and after implant-placement surgery

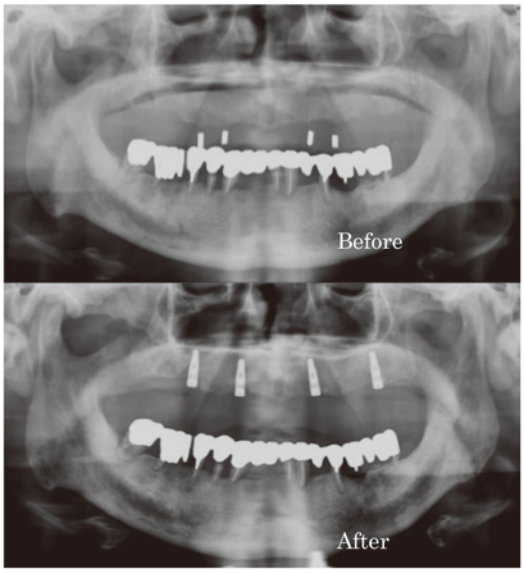

These panoramic X-ray images are from before and after implant implantation. Absorption of the maxillary alveolar bone is recognized; however, in March 2011, we implanted a 4.3 mm x 13 mm tapered implant at the maxillary bilateral canine tooth and the second molar tooth (17, 13, 23, and 27).

Therapeutic procedures

We surgically removed the stent for implantation with reference to the denture made at the first visit and after the first operation and second operation, since the outer mucosal symptoms on the buccal side of the second molar teeth on both sides were remarkable. After that, we observed the outcome while using mucosal conditioning material. For the final denture production, we made a pilot denture, duplicated it and attached the magnet structure to the denture after the metal floor denture was made, and completed it.

Working cast・Record base with occlusion rim・Wax denture

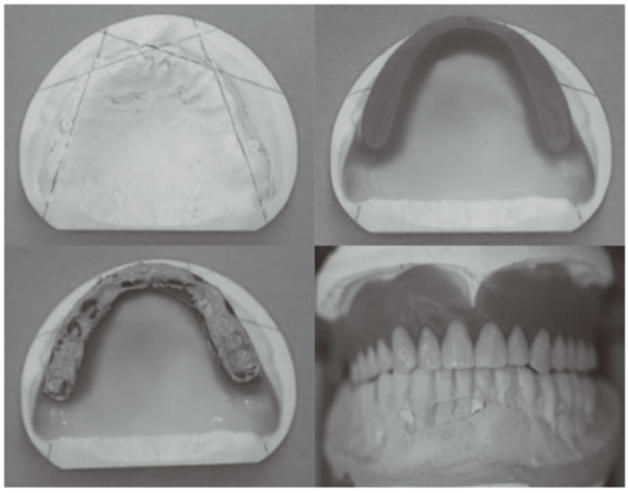

The pilot denture working model, the occlusal floor, and the crescent teeth are shown. The implant was placed in a good position by using the dental prostheses made at the initial visit for examining the implant placement position.

Wax denture・bite-seating impression・ finished denture

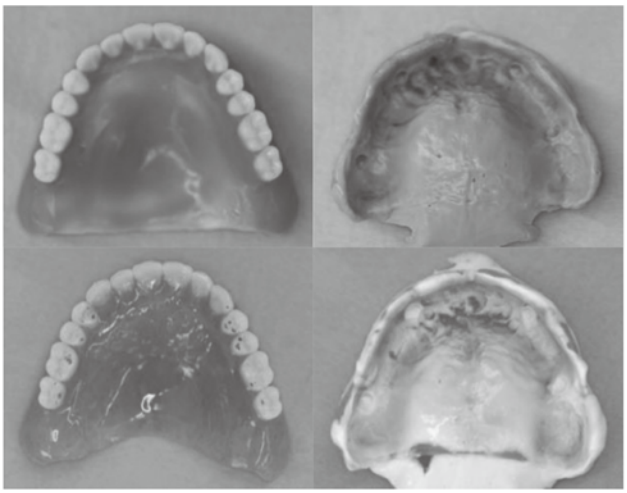

A crescent tooth and bite impression and a completed denture are shown. The fitting of the pilot denture was also good.

Mucosal surface-matching state

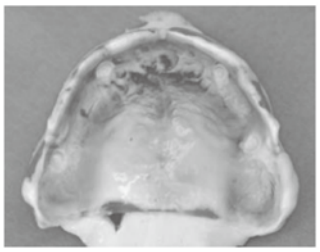

Installation of denture

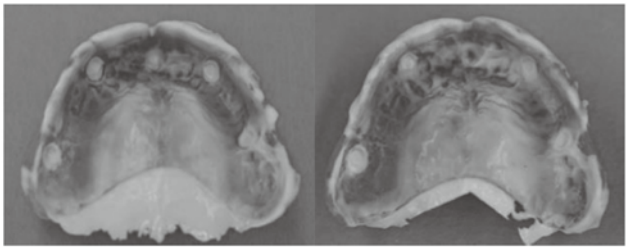

After 5 days After 15 days

The temporal course of the mucosal surface and the change in the conformity state at occlusion are shown. The compliant condition was improved after five and fifteen days of wearing the denture.

Impression of the pilot denture

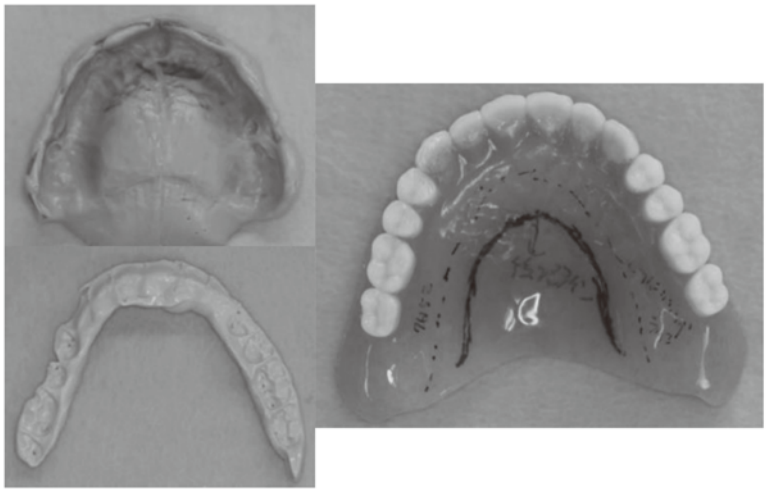

The bite-seating impression using the pilot denture is shown. The fitting and occlusion of the pilot denture were also good. Instructions on the finishing line and palate denture margin have been written in the bite-seating impression and the pilot denture.

Working cast and wax denture

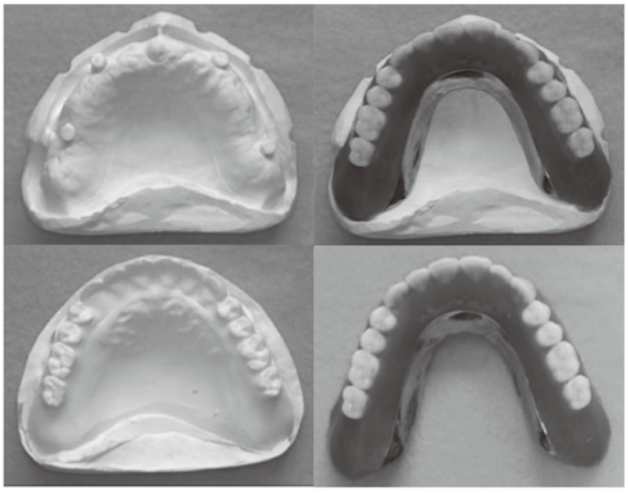

The working cast and wax denture are shown. A buccal side core, arrangement of the artificial teeth, and finished wax dentures were obtained.

Finished denture and the magnetic attachment placed on the denture

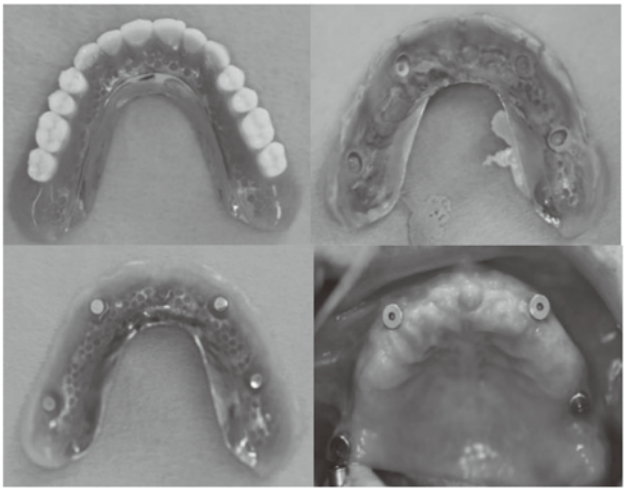

The impression for the finished denture and the magnetic attachment put on the denture are shown. From the thickness of the impression material, it can be seen that the fit of the denture is good. On the model, after injecting gypsum in the laboratory, the magnet structure was attached to the denture.

After denture insertion

The patient is shown after putting on the denture. The fitting and power maintenance of the denture was good, and the patient was also satisfied with the oral sensation of the palatal denture base. Due to the stabilization of the maxillary dental prosthesis, the bridge of the mandible had been worn for about two years and was confirmed to be flushed. After extraction of the tooth, it became a complete denture.

Three years and six months after
providing the patient with dentures

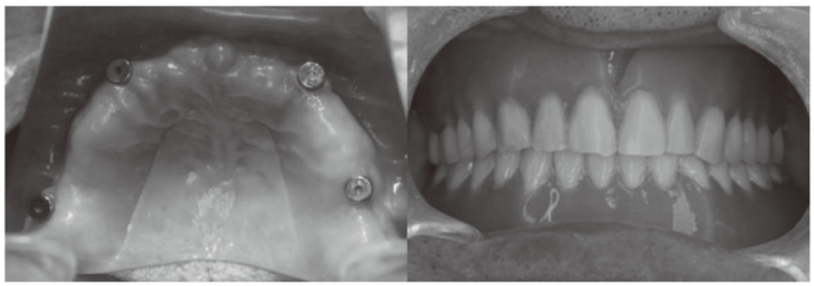

An intraoral photograph taken three years and six months later is shown. The occlusion was stabilized by making the lower jaw into a complete denture.

Four years and three months after
providing the patient with dentures

Photographs of the inside of the mouth and the dentures after four years and three months are shown. Although five years have not yet passed, I was pleased when the patient visited last month and was satisfied.

Discussion

It is difficult to adjust the amount of pressure on the implant in a well-balanced manner; in some cases, the attachment may not be adsorbed due to repulsion of the mucosal tissue. The Magfit SX2®, which was used this time, has a range of motion of 0.4 mm, which is close to the amount of pressure displacement of the mucosa. Furthermore, the denture was made in consideration of its characteristics and impression pressure control. Since the patient has functioned well now, even four years after its installation, this method seems to make it easy to balance the amount of implant displacement and mucosa pressure, even for dentists who do not have clinical experience.

A basic study on the accuracy of a zirconia coping fabricated by CAD/CAM system-Effect of abutment modification-

H. Hamasaka, M. Sone, Y. Okawa, S. Somekawa, S. Ueda, M. Masuda, A. Matsui, Y. Toyota, F. Narumi, T. Matsukawa, K. Okamoto, and S. Ohkawa
Division of Removable Prosthodontics, Department of Restorative and Biomaterials Sciences, Meikai University School of Dentistry

Abstract

The purpose of this study was to evaluate the influence of 2 different abutment tooth forms (for metal coping and CAD/CAM coping) on the fitting accuracy of zirconia coping. Zirconia copings were made of a semi-sintered zirconia block (Cercon® base, DeguDent) using the dental CAD/CAM system (Cercon® brain, DeguDent). Fitting accuracy was evaluated by a cement-replica technique with white and blue silicone materials. After the cement-replica specimens were sectioned, the thickness of the cross-sectioned white silicone layer was measured at 5 points. For zirconia coping specimens, the mean discrepancy of fitting gaps was over 120 μm between the die and the zirconia coping at all points in each group. This study suggested that the zirconia coping fabricated by this system requires more precise fitting accuracy.

Introduction

The dental CAM system and CAD/CAM system has been used generally to fabricate various prostheses in clinical dentistry. The progress of dental CAD/CAM technology has made it possible to use high-strength ceramic materials such as zirconia, and zirconia ceramics have become popular materials in clinical dentistry. Zirconia ceramics have excellent mechanical strength for prosthetic appliances and are biocompatible with a significant reduction in plaque.[1] These facts suggest that zirconia ceramics are clinically useful for keeper copings of magnetic attachments.

Nevertheless, the keeper copings of magnetic attachments were still cast by the lost wax method used in dental casting. Our present study[2] introduced the method of zirconia keeper copings fabricated by the dental CAM system. However, the adaption had poorer clinical acceptability than did other prostheses. Thus, we prepared 2 different abutment tooth forms for zirconia keeper copings and investigated the fitting accuracy.

The purpose of this study was to evaluate the influence on fitting accuracy of 2 different abutment tooth forms of zirconia copings fabricated by the same CAD/CAM system.

Materials and Methods

Materials: The prepared epoxy resin lower canine tooth (338: NISSIN) was selected as the abutment tooth. The abutment tooth forms for the metal coping (MC) and the abutment tooth form for the CAD/CAM coping (CC) are shown in Figs. 1 and 2. As compared to the abutment tooth form for MC, the rotational resistance groove was removed for the CC, giving additional reduction to gain more clearance and rounding all orifice line angles.

The keeper copings were fabricated using the dental CAD/CAM system (Cercon® brain, DeguDent), and a semi-sintered zirconia block (Cercon® base, DeguDent) was employed for the keeper coping material (Table 1).

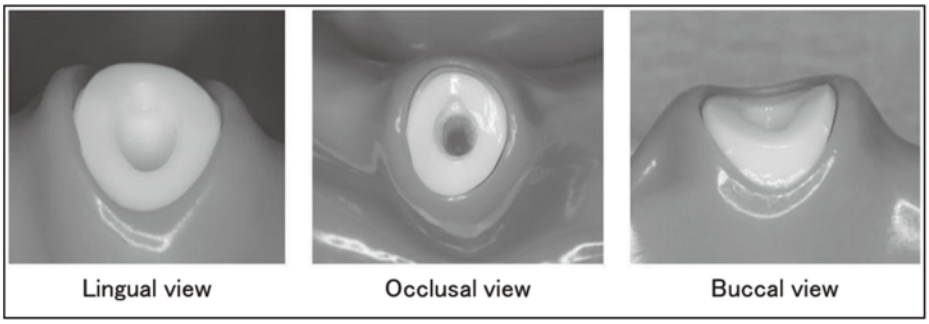

Fig. 1 Abutment tooth form for the MC

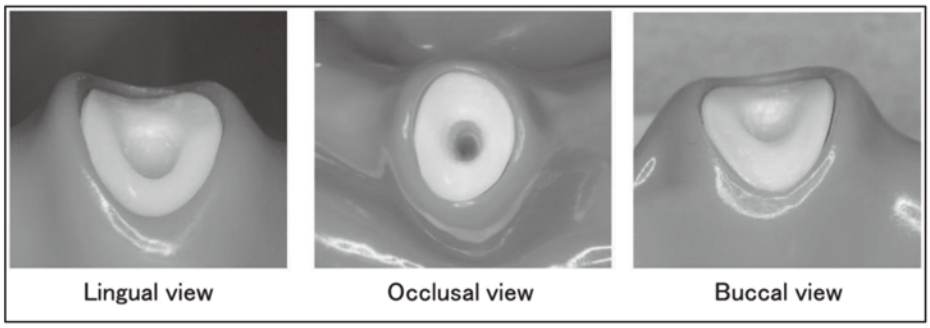

Fig. 2 Abutment tooth form for the CC

Puroduct	Composition
Cercon® base	ZrO_2 89.2%
	Y_2O_3 5.0%
	HfO_2 5.0%
	other oxides

Table 1 Material composition

Methods (*Cement-replica technique*): Fitting accuracy was evaluated using a cement-replica technique. Each keeper coping was placed in the master die with a white silicone material (FIT CHECKER ADVANCED, GC). After curing the white silicone material, the keeper coping with the white silicone material was removed from the master die. Then, the keeper coping with it was embedded in a blue silicone material (EXAMIXFINE Regular Type, GC). The keeper coping was demounted from the cured silicone material, and a blue silicone material filled in the space (Fig.3).

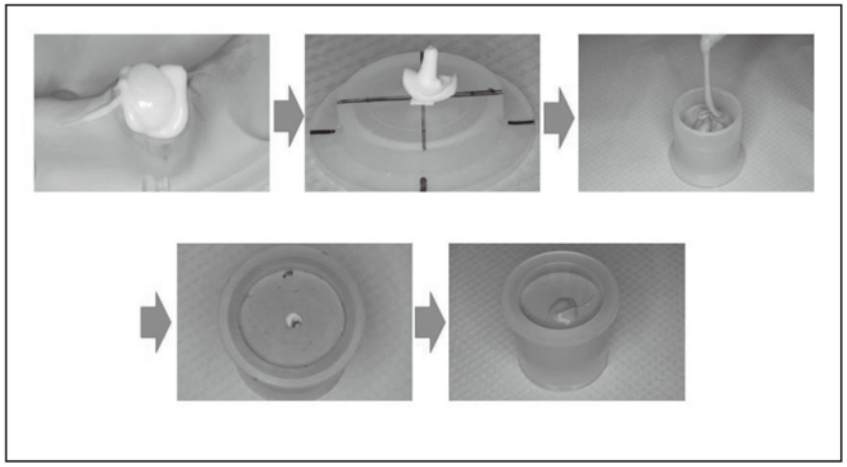

Fig. 3 Procedure for fabricating specimens (cement-replica technique)

Determination of fitting accuracy: Each silicone-replica specimen was sectioned in the buccolingual direction through the center of the coronal root. The measuring points of the white silicone layer are shown in Fig.4. The thickness of the white silicone layer was measured at each point (a: canal orifice of the lingual wall; b: center of the lingual wall; c: apical part of the post; d: center of the buccal wall; e: canal orifice of the buccal wall).

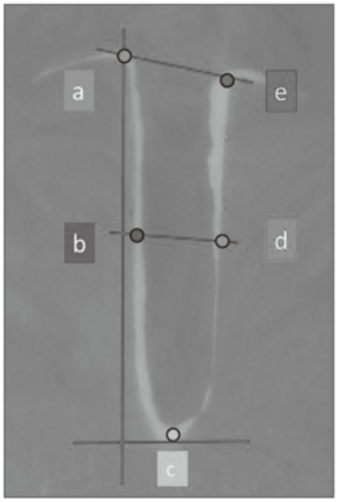

Fig. 4 Locations of the measuring points

Results

The mean thicknesses of the white silicone layer, namely the mean fitting gaps, were 781 ± 79 μm at point a, 167 ± 69 μm at point b, 193 ± 31 μm at point c, 168 ± 58 μm at point d, and 156 ± 46 μm at point e in the MC group (Fig.5). There were statistically significant differences between point a and other measuring points by one-way ANOVA and the Tukey–Kramer method ($p<0.05$).

In the CC group, the mean fitting gaps were 300 ± 147 μm at point a, 171 ± 19 μm at point b, 250 ± 67 μm at point c, 127 ± 43 μm at point d, and 192 ± 129 μm at point e (Fig.6). There were no significant differences in the mean thicknesses of the white silicone layers between the 5 measuring points by one-way ANOVA and the Tukey–Kramer method ($p<0.05$).

Application of the Student *t*-test indicated that there was a statistically significant difference between the MC and the CC groups at point a (Fig.7).

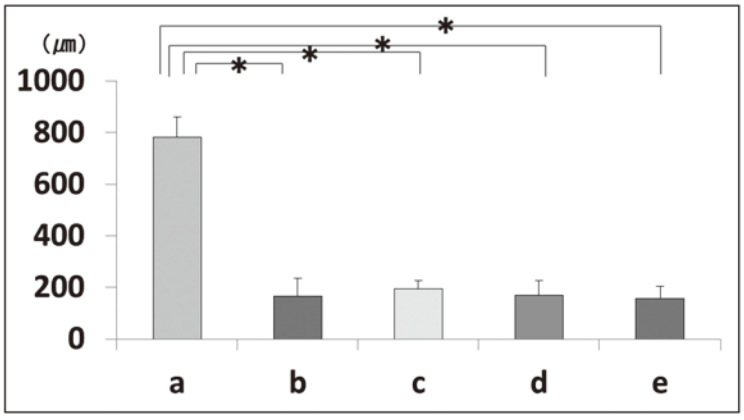

Fig. 5 Mean thicknesses of the white silicone layers at 5 measuring points (MC)

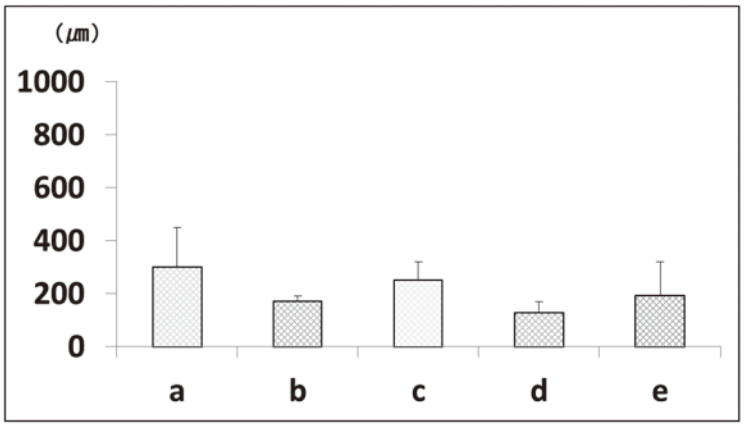

Fig. 6 Mean thicknesses of the white silicone layers at 5 measuring points (CC)

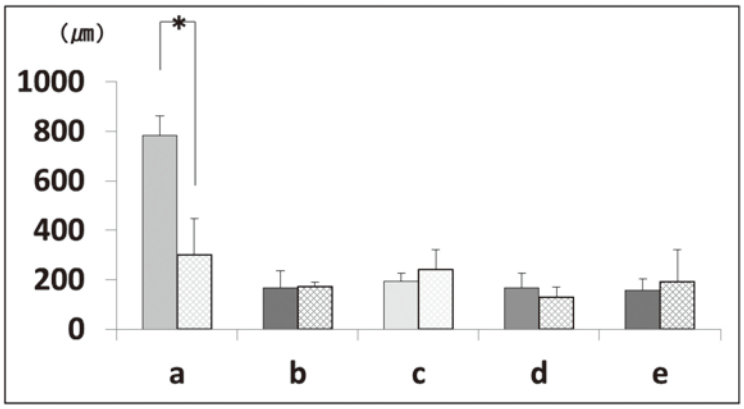

Fig. 7 Mean thicknesses of the white silicone layers at 5 measuring points in both groups

Discussion

Within the limitations of this study, it was concluded that modification of the abutment tooth form improved fitting accuracy at point a in this system. This result indicates that removing rotational resistance grooves and rounding all orifice line angles could have influenced the fitting accuracy of point a. However, the fitting accuracy of a zirconia keeper coping fabricated by this system, ether MC or CC, had unacceptable marginal gaps of 100 μm.[3] This result suggests that the adaptation of a zirconia keeper coping fabricated by this system is not clinically recommended. Further investigation is needed to fabricate CAD/CAM keeper copings.

References

1. T. Miyazaki, T. Nakamura, H. Matsumura, S. Ban, and T. Kobayashi: Current status of zirconia restoration, J Prosthodont Res, 57, 236–261, 2013.
2. H. Hamasaka, M. Sone, Y. Okawa, S. Somekawa, M. Masuda, A. Matsui et al.: A basic study on the fitness of a zirconia keeper coping fabricated by the CAM system, J J Mag Dent, 25(2), 24–26, 2016.
3. N. Suto, S. Miura, R. Inagaki, M. Yoda, and K. Kimura: A Basic Study on Fitness of All-ceramic Crown Fabricated by CAD/CAM system, Ann Jpn Prosthodont Soc, 1, 21–28, 2009.

A basic study on the accuracy of a zirconia coping fabricated by the CAD/CAM system -Application for post scanning-

S. UEDA, M. SONE, M. HAMASAKA, Y. OKAWA, S. SOMEKAWA, M. MASUDA, A. MATUI, Y. TOYOTA, F. NARUMI, T. MATSUKAWA, K. OKAMOTO, and S. OHKAWA

Division of Removable Prosthodontics, Department of Restorative and Biomaterials Sciences, Meikai University School of Dentistry

Abstract

The purpose of this study was to evaluate the fitting accuracy of zirconia keeper copings manufactured by computer-aided design and manufacturing using scan posts.

The keeper copings, made from a zirconia block, were fabricated with four different cement spaces as specimens (n=3 for each). The fitting accuracy of the specimens was evaluated using the cement replica technique. Each silicone replica specimen was sectioned in the buccolingual direction through the center of the coronal aspect of the root. The thickness of the white silicone layer was examined at five measuring points (A: canal orifice of the lingual wall, B: center of the lingual wall, C: apical part of the post, D: center of the labial wall, E: canal orifice of the labial wall).

The mean thickness of the white silicone layer at the five measuring points was 81±22, 239±39, 574±68, 223±43 and 67±19 μm for points A, B, C, D and E, respectively. There was no significant difference between the results for each cement space ($P<0.05$).

Within the limitations of this study, it was suggested that the fitting accuracy of zirconia keeper copings manufactured with this CAD/CAM system using scan posts was within the clinically acceptable range, excluding marginal gaps.

Introduction

Advancements in computer-aided design/computer-aided manufacturing (CAD/CAM) techniques have improved prosthetic devices milled in the dental clinic and laboratory. With CAD/CAM techniques, copings and frameworks for all-ceramic restorations can be made from zirconia. This material has high stability and toughness. Digital impression systems are generally composed of a three-dimensional scanner recording the object and CAD software that uses the scanned image to design the prosthesis.

Although a method for manufacturing CAD/CAM keeper copings using a scanning probe has been reported[1),] the keeper coping of the magnetic attachment was still manufactured using the lost-wax casting method.

Recently, laser scanning using a dental CAD/CAM system has been primarily used for producing zirconia prostheses because of its high-precision performance. However, there is greater distortion of the digital impression when scanning a prepared root canal, possibly because of the limitations of the specific scanning technology. Although applying a scan post could enable digital images of the prepared root canal to be obtained, there have been no studies investigating this method.

The purpose of this study was to evaluate the fitting accuracy of zirconia keeper copings manufactured by CAD/CAM using scan posts.

Materials and Methods

Keeper coping fabrication

Prepared epoxy resin mandibular canine teeth (338; Nissin) with a root canal length of 5.0 mm were selected as abutment teeth for the keeper copings. Impressions were taken of the prepared teeth using silicone impression material (Examixfine Regular Type, GC). The working casts were made of type IV gypsum (New Fujirock, GC). A scan post (Scan Posts, 3Shape) was placed into the prepared post space on each working cast (Fig. 1). The keeper copings were designed using CAD software (Dental Designer, 3Shape) after digitalization of the die was performed using a laser scanner (Aadva Scan D850, GC).

The keeper copings, made from a zirconia block (Aadva Zirconia Disk, GC), were fabricated with four different cement spaces as specimens (Fig. 2). Each cement space for the zirconia copings was fabricated using a milling machine (GM-1000, GC).

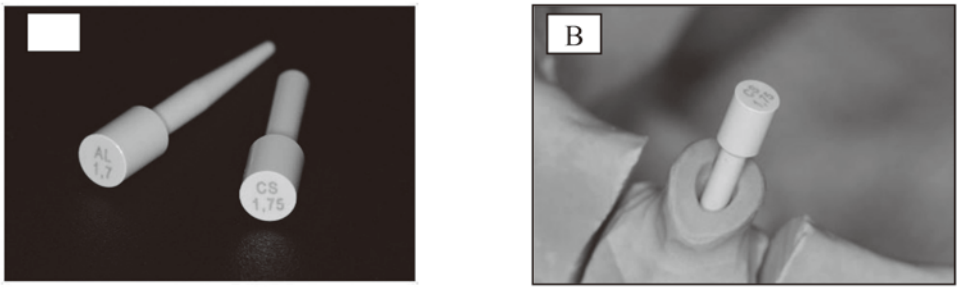

Fig. 1 Scan post placed into the prepared root canal on the master die
(A. Scan posts, B. Insert into the master die)

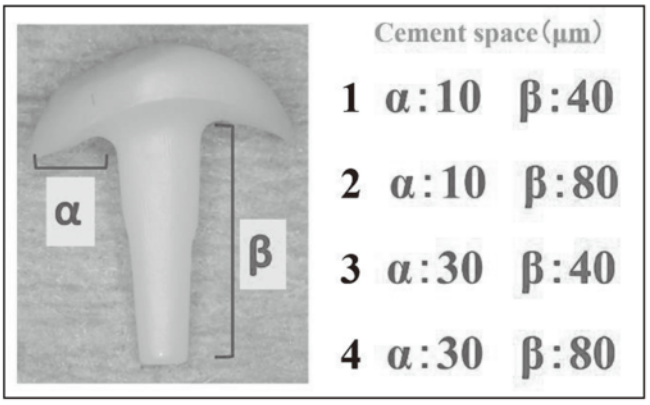

Fig. 2 Four different cement spaces

Cement replica technique

The fitting accuracy was evaluated using a cement replica technique. The post space was filled with a white silicone material (Fit Checker Advanced, GC) and the keeper coping was seated on the master die using finger pressure. After curing the white silicone, the keeper coping and white silicone material were removed from the master die. These keeper copings were then embedded in a blue silicone material (Examixfine Regular Type, GC) and the space created by demounting the keeper copings from the cured silicone material was filled by the blue silicone (Fig. 3).

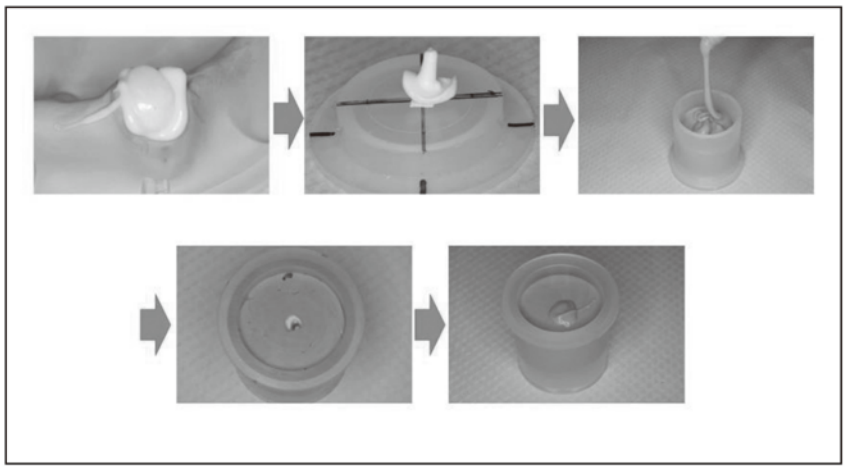

Fig. 3 Fabrication of the specimens (cement replica technique)

Fitting accuracy

The silicone replica specimens were sectioned in the buccolingual direction through the center of the coronal aspect of the root (Fig. 4). The thickness of the white silicone was determined as a measure of the discrepancy between the die and the restoration. The distances were recorded at five different measuring points. The measuring points are defined in Fig. 5.

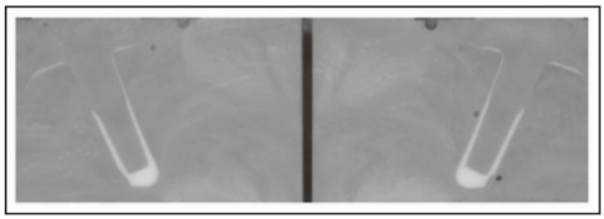

Fig. 4 Silicone replica specimen sectioned in the buccolingual direction

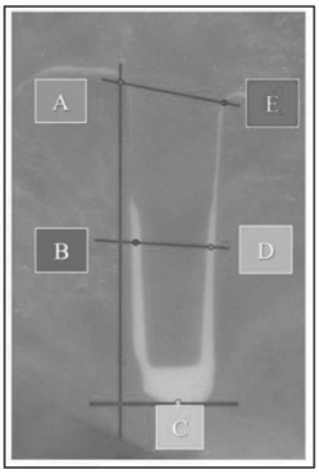

Fig. 5 Measuring points
(A: canal orifice of the lingual wall, B: center of the lingual wall, C: apical part of the post, D: center of the labial wall, E: canal orifice of the labial wall)

Statistical analysis

The fitting accuracy at the different measuring points was analyzed statistically using one-way analysis of variance and post hoc Scheffé test (P<0.05).

Results

The mean thicknesses of the white silicone were 81±22, 239±39, 574±68, 223±43 and 67±19 μm for points A, B, C, D and E, respectively. Point C had significantly higher values as compared to the other measuring points (Fig. 6).

There were no statistically significant differences among the different cement spaces.

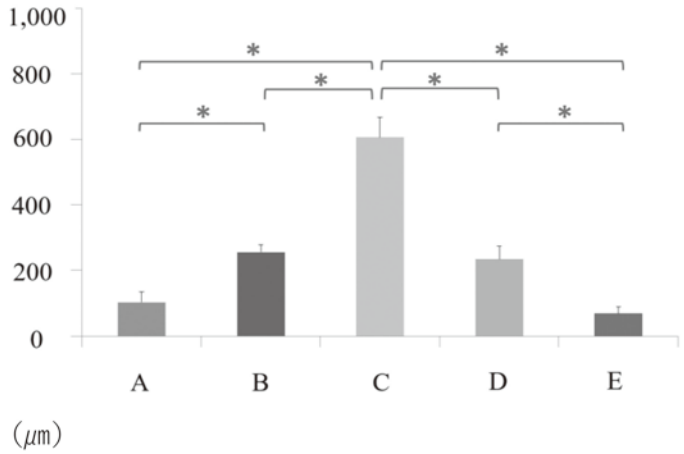

Fig. 6 Thicknesses of the white silicone layers at five measuring points

Discussion

Suto et al. reported that the clinically acceptable limit for the fitting accuracy of CAD/CAM restorations is a discrepancy up to 100 μm[2)].

The gaps at point B, C and D had higher values when compared with the clinically acceptable range. However, there was a possibility that the fitting accuracy achieved was within the clinically acceptable range because of modifications to the spacer setting on the CAD software.

The mean of the internal gaps at points A and E in this study ware within 100 μm. The fitting accuracy of the zirconia copings fabricated using the scan posts method was within the clinically acceptable range when excluding marginal gaps.

The fitting accuracy of the marginal gaps in the keeper copings manufactured with this CAD/CAM system should be examined in future studies.

Conclusion

Within the limitations of this study, it was suggested that the fitting accuracy of zirconia keeper copings manufactured with this CAD/CAM system using scan posts was within the clinically acceptable range, excluding marginal gaps.

References

1. K. Tsuda, Y. Tanaka, T. Kanazawa, M. Sakane, and K. Kumano: Fabrication of a keeper coping by use of the CAD/CAM system, J J Mag Dent, 13(1), 9–17, 2004.
2. N. Suto, S. Miura, R. Inagaki, M. Yoda, and K. Kimura: A basic study on fitness of all-ceramic crown fabricated by CAD/CAM system, Ann Jpn Prosthodont Soc, 1, 21–28, 2009.

25 mm

25 mm

How to Write the proceedings

25 mm

0.5 line

TiTle including No. : Times New Roman 14pt Bold

Name (Initial. Family name) : Times New Roman 11 pt, (indent of a 0.5 line above and under this line)
ex. Y. Takada, N. Takahashi[1] and O. Okuno[2]

0.5 line

Affiliation: Times New Roman 11 pt, ex. Division of Dental Biomaterials, Graduate School of dentistry, Tohoku University
[1]Depatrtment of Magnet Science, School of Dentistry, Inaka College
[2]Laboratry of Magnet, Institute of Sendai

One line

0.5pt line (Black)

0.5 line

Abstract: Times New Roman bold 11 pt. Type
Abstract should be 10.5 point type (fonts such as Times New Roman (for body text) and Arial(for Headlines) are easy to read)

0.5pt line (Black)

One line

0.5 line

Manuscript Basics

The proceedings book will be printed directly from the manuscript provided by the author. The conference secretariat staff does not edit or proofread manuscripts, so all material should be concise and error free. The entire paper must be legible.

The components of a paper are (in order of appearance)

Introduction
Objective
Materials and Methods
Results or (Results and discussion)
Discussion
Conclusion
Acknowledgements
References

One line

Manuscripts Should

0.5 line

- be in a one-column format
- be 10.5 point type (fonts such as Times New Roman (for body text) and Arial(for Headlines) are easy to read)
- be single-spaced
- be justified within the column
- be written by the standard format of MS Word 2003 (number of characters and lines in a page)

Authors should use the page size of A4 format (210 mm × 297 mm). Four spaces (half size English character) should be inserted in the head of first line between paragraphs.

Main Headings

- bold 12 pt. Type
- 12 pts. (1 line space) before and 6 pts. (0.5 line space) after
- upper- and lower-case
- NO underline (underscore)
- NO italic
- one line of space above and below, except when the heading is at the top of a column
- left justified

Subheadings

- be bold 10.5 pt. type (font: Arial)

25 mm

- upper and lowercase
- NO underline (underscore)
- NO italic
- indented and on-line with the rest of the paragraph (no extra space above and below)
- *Secondary Subheadings*
- italic 10.5 pt. type (font: Arial)
- upper and lowercase
- NO underline (underscore)
- NO bold
- indented and on-line with the rest of the paragraph (no extra space above and below)

Margins

- Top 25 mm
- Bottom 25 mm
- Left and right 25 mm

Figures and Tables

All figures and tables should be imported directly into the document and will be printed along with the text. Figures and tables will NOT be reduced or enlarged by the conference secretariat staff. All figures and tables will be printed in black and white, so do not refer to colors within text to describe graph lines or particular areas of photos.

However, if you will demand the PDF file of your manuscript, you may use colors because the PDF file refer to colors. Note, however, that you should use colors which can be distinguished even when they are printed in black and white.

All figures and tables should be numbered consecutively and placed in numerical order within the manuscript. For each figure, a caption should be placed directly below the figure, and should include the figure number and caption text.

References

Literature references should be listed at the end of the paper in the same order that they appear in the text, and in accordance with the following examples.

1. Journal article (example): Y. Takada, N. Takahashi and O. Okuno: Electrochemical behavior and released ions of the stainless steels used for dental magnetic attachments, J J Mag Dent, 16(2), 49-52, 2007.
2. Book (example): R. Kunin, On Exchanging Resins, pp 88, Robert E. Kreiger Publishing Company, New York, 1972.